Heliyon 10 (2024) e27525

Contents lists available at ScienceDirect

Heliyon

journal homepage: www.cell.com/heliyon

Research article

Aspongopus chinensis Dallas induces pro-apoptotic and cell cycle arresting effects in hepatocellular carcinoma cells by modulating miRNA and mRNA expression

Renlian Cai [a,b,1], Xumei Chen [a,1], Samiullah Khan [a,1], Haiyin Li [a], Jun Tan [b], Ying Tian [b], Shuai Zhao [a], Zhiyong Yin [a], Daochao Jin [a,**], Jianjun Guo [a,*]

[a] *Provincial Key Laboratory for Agricultural Pest Management of Mountainous Region, Institute of Entomology, Guizhou University, Guiyang, Guizhou, 550025, China*

[b] *Department of Histology and Embryology, Zunyi Medical University, Zunyi, Guizhou, 563000, China*

ARTICLE INFO

Keywords:
Aspongopus chinensis Dallas
Inhibitory effect
Hepatocellular carcinoma
High throughput sequencing
miRNA-mRNA network interaction

ABSTRACT

Aspongopus chinensis Dallas is a traditional Chinese medicinal insect with several anticancer properties can inhibit cancer cell growth, by inhibiting cell division, autophagy and cell cycle. However, the precise therapeutics effects and mechanisms of this insect on liver cancer are still unknown. This study examined the inhibitory influence of *A. chinensis* on the proliferation of hepatocellular carcinoma (HCC) cells and explore the underlying mechanism using high-throughput sequencing. The results showed that *A. chinensis* substantially reduced the viability of Hep G2 cells. A total of 33 miRNAs were found to be upregulated, while 43 miRNAs were downregulated. Additionally, 754 mRNAs were upregulated and 863 mRNAs were down-regulated. Significant enrichment of differentially expressed genes was observed in signaling pathways related to tumor cell growth, cell cycle regulation, and apoptosis. Differentially expressed miRNAs exhibited a targeting relationship with various target genes, including *ARC*, *HSPA6*, *C11orf86*, and others. Hence, cell cycle and apoptosis were identified by flow cytometry. These findings indicate that *A. chinensis* impeded cell cycle advancement, halted the cell cycle in the G0/G1 and S stages, and stimulated apoptosis. Finally, mouse experiments confirmed that *A. chinensis* significantly inhibits tumor growth *in vivo*. Therefore, our findings indicate that *A. chinensis* has a notable suppressive impact on the proliferation of HCC cells. The potential mechanism of action could involve the regulation of mRNA expression via miRNA, ultimately leading to cell cycle arrest and apoptosis. The results offer a scientific foundation for the advancement and application of *A. chinensis* in the management of HCC.

1. Introduction

Aspongopus chinensis Dallas (Hemiptera: Dinidoridae), traditional medical insect, has several nutritional and medicinal properties with high level of different amino acids [1]. This insect has several anticancer qualities and is often found in China and Southeast Asia

* Corresponding author.
** Corresponding author.
E-mail addresses: daochaojin@126.com (D. Jin), jjguo@gzu.edu.cn (J. Guo).
[1] These authors contributed equally to the manuscript.

https://doi.org/10.1016/j.heliyon.2024.e27525
Received 8 November 2023; Received in revised form 29 February 2024; Accepted 1 March 2024
Available online 7 March 2024

[2]. In earlier studies, evidence has been presented to support several health advantages associated with the use of this insect, particularly in relation to its anti-cancer, anti-bacterial, and anti-clotting properties [3–6]. Thus, its diverse properties highlight the crucial role of this valuable insect as a cultural, medicinal, and economic resource. The demand for this insect has increased dramatically over the last several years. Moreover, *A. chinensis* presents anticancer properties and has been identified as a herbal remedy to treat tumours. *A. chinensis* is principally used in the treatment of kidney diseases, the removal of blood stasis, and improvement of fatigue [7,8]. Generally, it is converted into a chemically stable decoction for use in TCM [9]. *A. chinensis* decoction (ACD) can inhibit cancer cell growth, including breast and liver cancer, by inhibiting cell division, autophagy, and apoptosis [10,11]. Several Chinese studies demonstrated that this insect partially protects mice from manganese-induced reproductive harm by activating antioxidant enzymes and inhibiting apoptosis-related gene expression levels [12,13]. Recent studies have shown that *A. chinensis* represents an essential anticancer component of TCM [14,15]. In addition, multiple non-peptide small compounds represent possible therapeutic candidates for reducing renal fibrosis and preventing extracellular matrix production in mesangial cells in patients with diabetes. These molecules also function as powerful inhibitors of Smad3 phosphorylation [16,17].

Liver cancer is a significant worldwide health concern, since its prevalence is on the rise. GLOBOCAN 2020 predicts 1.4 million new cases and 1.3 million deaths from liver cancer by 2040, a 56.4% increase from 2020 [18]. Hepatocellular carcinoma (HCC) is the most common type of liver cancer [19]. However, due to the complexity of the HCC tumour microenvironment, its chemotherapeutic efficacy is very low [20,21]. Traditional Chinese medicine (TCM) provides several benefits over other related medical practises for HCC [22], especially its effect on multiple cancer-related signalling pathways and molecular targets [7]. TCM has several anticancer properties, including inhibiting proliferation, regulating immunological response, and inducing apoptosis [23]. These positive aspects of TCM implies that it could be a potential therapeutic strategy for treating cases with a range of malignancies [24,25]. However, the mechanisms of action have not been fully investigated and require further research.

MicroRNAs (miRNAs) are small endogenous RNAs consisting of 19–22 nucleotides. miRNAs serve as a critical regulator of post-transcriptional genes [26] by destabilising target mRNAs and preventing their translation by binding to their 3′-untranslated regions [27]. The dysregulated function of these RNAs is connected to numerous diseases, such as cancer and autoimmune disorders [28,29]. Recent studies have made considerable advancements in investigating small RNAs, with special focus on miRNA functions, including development, metabolism, and reproductive pathways [30–32]. In human diseases, the aberrant regulation of microRNAs influences their normal function. A correlation has been observed between cancer prognosis and alterations in cellular miRNA expression in malignant tissues and extracellular miRNA expression in exosomes. Hence, miRNAs can be employed in numerous clinical applications as cancer biomarkers and therapeutic targets [33]. Moreover, aberrant regulation of these miRNAs may possibly promote the initiation of cancers [34,35]. Several miRNA–mRNA interaction network analyses have revealed that miRNAs can target multiple target genes and may be regulated by multiple miRNAs [36]. Thus, miRNAs are potential therapeutic targets as well as biomarkers.

Although *A. chinensis* is considered a promising anti-HCC therapy, extensive experimental studies on *A. chinensis* are lacking owing to its complex chemical composition and unknown mechanisms of action. To investigate the molecular mechanism by which *A. chinensis* inhibits the proliferation of HCC cells, the expression profiles of miRNA and mRNA were analysed.

2. Materials and methods

2.1. Cell culture

In Minimum Essential Medium and Eagle's modified Dulbecco's medium, Hep G2 and Hepa 1–6 cells (Chinese Academy of Sciences) were cultured separately, including 10% (v/v) foetal bovine serum (GE HealthCare, Chicago, IL, USA) and 1% (v/v) penicillin–streptomycin solution, in an incubator Aat 37 °C and 5% CO_2.

2.2. Aspongopus chinensis decoction (ACD) preparation

Adult *A. chinensis* specimens were collected from Kaili City, Guizhou Province, China, The specimens were authenticated by Prof. Zizhong Li (Institute of Entomology, Guizhou University, Guiyang, China) and the genome was sequenced (the accession number PRJNA729875) [37]. and maintained at −80 °C. The preparation of ACD was conducted using the methodology outlined by Tian et al., and the primary compound composition was identified through GC-MS technology [38]. Samples were dried, rinsed in deionized H_2O thrice, and powdered. Subsequently, they were mixed in a ratio of 100 mL of deionized water and 50 g of insect powder and then soaked for 30 min. The powdered insect specimens were first decocted for 1 h and then further decocted at low heat to achieve a concentration of 1 g/mL. The resultant liquid was filtered through gauze and then filter paper before being centrifuged at 6000 g for 10 min and sterilised using a 0.22 μm filter (Burlington, Massachusetts, USA). The decoction was maintained at 20 °C until use.

2.3. Cell viability assay

A Cell Counting Kit 8 assay (HB-CCK-8-500, Hanbio, Shanghai, China) was used to measure Hep G2 cells viability. Briefly, 8×10^4 cells/well were inoculated into 96-well plates. Then, various concentrations of ACD (20, 30, or 40 mg/mL) were added in six replicate wells (100 μL/well). The control wells included complete medium solution. After incubating the cells for 24 h, 48, or 72 h, 90 μL of medium was added to each well followed by 10 μL of CCK-8 reagent. After 2 h incubation, the absorbance at 450 nm was measured using an automated microplate reader. The formula used for cell viability was as follows:

Cell viability (%) = $(A2 - A1) / (A3 - A1)) \times 100\%$ [39],

where *A1, A2, and A3* represent the OD values of the blank, experimental, and control wells, respectively.

2.4. Cell cycle phase assessment

In 6-well dishes, 2×10^5 cells Hep G2 cells were seeded for 24 h. Various ACD concentrations (20, 30, or 40 mg/mL) were applied to incubate these cells. Trypsinisation with EDTA-free trypsin (Promega, Madison, WI, USA) was used to extract these cells, which were then fixated for 12 h at 4 °C with 70% ice-cold ethanol and centrifuged for 5 min at 1000×*g*. Next, the collected pellet was washed twice with ice-cold PBS and 200 L of cell cycle detection reagent was added. After staining cells in the dark for 30 min at 37 °C, flow cytometry was used to analyze cell cycle.

2.5. Cell apoptosis assay

The apoptosis rate was further analysed via the Annexin V-FITC Apoptosis Detection Kit (KGA1101-100, Nanjing KeyGen Biotech, China). Cells were inoculated in 6-well plates for 24 h before being treated with ACD at concentrations of 20, 30, or 40 mg/mL.

The cells were subsequently extracted, rinsed twice with ice-cold PBS, and suspended in 500 μL buffer. A 5 μL Annexin V-FITC solution was added to the cell suspension along with 5 μL propidium iodide. Fluorescence was measured by flow cytometry after 15 min at 25 °C in the dark.

2.6. RNA extraction

We treated Hep G2 cells with the IC50 concentration of ACD for 24 h, and the contents of the control cells were harvested. Three replications were performed. Cells in the control group were only cultured in complete culture media. RNA was isolated and purified using TRIzol reagent.

2.7. Small RNA library construction and sequencing

Using polyacrylamide gel electrophoresis, small RNAs (18–30 nucleotides) were extracted from total RNA. After ligation of the 5′ and 3′ adapters, reverse transcription and amplification of RNA were performed. The libraries were analysed for size and purity on a 2100 Bioanalyzer, sequenced on a BGISEQ-500 platform, and processed using MGISEQ-2000RS sequencing technology (MGI Tech, Shenzhen, China).

2.8. RNA sequencing

BGISEQ-500 sequencing technology was used for miRNA sequencing. The original data were contaminated and contained numerous readings with a high proportion of unknown bases N, which were eliminated prior analysis to ensure the results' validity. After obtaining clean reads, Bowtie 2 was utilized to compare them to the human genome (GCF_000001405.38_GRCh38.p12) [40].

2.9. Sequencing data analysis

The sequence of miRNA from samples and results predicted by the existing miRNA database were compared, and the expression of miRNA was determined. To compare the sample expression, and identify the differentially expressed miRNAs, we utilized DESeq2 [41]. The filtering criteria were specified as $|\log2FC| \geq 2$ and q-value ≤ 0.05.

2.10. MiRNA-target gene prediction

To predict target genes, RNAhybrid [42], miRanda [43], and TargetScan [44] were applied. By combining free energy and score values, target genes were then filtered.

2.11. Gene Ontology (GO) and Kyoto Encyclopaedia of Genes and Genomes (KEGG) analyses of target genes

Using the GO database (http://geneontology.org), target genes of differentially expressed miRNAs were assigned GO functional annotations. In addition, the signalling pathways associated with target genes were also annotated based on the KEGG database (https://www.genome.jp/kegg/).

2.12. Construction of differentially expressed miRNA and target gene networks

Target mRNAs were predicted based on the differential expression of miRNAs ($|\log2FC| \geq 3$, q-value ≤ 0.001). The miRNA–mRNA interaction network was then visualized.

2.13. qRT-PCR

The poly(A)-tailed RT-PCR was used to validated four differentially expressed miRNAs [45]. A miRcute Plus miRNA First-Strand cDNA Kit (KR211, Tiangen, Beijing, China) was used to reverse-transcribe total RNA extracted from cells by adding poly(A) tail to the 3 'end of the miRNA. Subsequently, PCR was performed using miRcute Plus miRNA qPCR Kit (FP411, Tiangen, Beijing, China) with a miRNA-specific forward primer and a universal primer. The subsequent procedures were carried out according to the manufacturer's instructions. The miRNA-specific forward primer used were as follows: hsa-miR-4485-3p: 5′-GCTAACGGCCGCGGTACCCTAA-3′; hsa-miR-214-3p: 5′-ACAGCAGGCACAGACAGG-3′; hsa-miR-26a-1-3p: 5′-GCGCCAGGCCTATTCTTGGTTACTTGC-3′; hsa-miR-92a-1-5p: 5′-GCAGGTTGGGATCGGTTGCAATGCT-3′; U6: 5′-TGCTCGCTTCGGCAGCACATATACT-3′. *U6* was used as the reference gene, and all reactions were repeated three times. The $2^{-\Delta\Delta Cq}$ method was used to compute the relative expression.

2.14. Animal experiments

Twenty-four male BALB/c mice (6–7 weeks age and 18 ± 2 g weight) from Byrness Weil Biotech (Chongqing, China) were housed at 20 ± 2 °C. The Animal Care and Use Institutional Committee of Guizhou University approved animal procedures under approval number EVE-GZU-2022-E044.

2.15. Anti-tumour activity of A. chinensis in vivo

The construction of the tumor model followed the methods described by Chen et al. [46]. A Hepa 1–6 cell suspension (1×10^7 cells/mL) was prepared. Subsequently, 200 μL of the suspension was subcutaneously injected into the axillary region of the animals. After 10 d, tumours (approximately 40 mm^3) were observed in the injected area. The mice were categorized into 4 groups (n = 6/group): positive control (sorafenib, 30 mg/kg), negative control (normal saline), ACD (ACD, 20 mg/mL), and combination group (ACD, 20 mg/mL; sorafenib, 30 mg/mL). The method and dose of sorafenib gavage were based on those commonly used in mice models [47]. Mice in each group received the corresponding drug via gavage daily for 14 days. At 2-d intervals, body weight (BW) and tumour volume were measured, and changes in tumour volume were computed. The tumour length and width were measured, and tumour volumes were determined using the following formula:

$V = (L \times W^2) / 2$ [48],

where *V, L,* and *W* represent the tumour volume, length, and width, respectively. Subsequently, on the 15th day, the mice were euthanized through cervical dislocation [49]. Tumour masses were determined.

2.16. Statistical analysis

The data were displayed as the mean standard deviation (mean SD) and analysed with one-way ANOVA plus Tukey's multiple comparisons test using GraphPad Prism 8.0 software. Statistical significance was determined at $P < 0.05$.

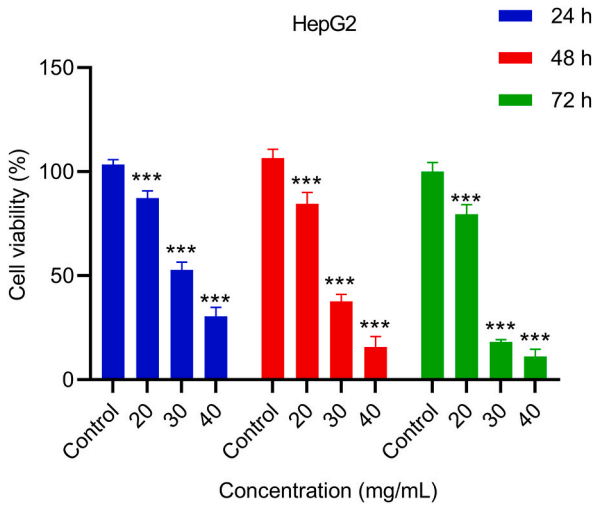

Fig. 1. Determination of HepG2 cell viability after exposure to various concentrations of ACD using a Cell Counting Kit 8 assay; (***P < 0.001).

3. Results

3.1. HepG2 cell viability

Hep G2 cells were treated with different concentrations of ACD (20, 30, or 40 mg/mL) to determine its effect on cell viability (Fig. 1). A significant reduction in the cell viability relative to the control group was observed ($P < 0.001$). A substantial reduction in cell viability was also observed over time after ACD treatment. An IC50 of 31.65 mg/mL was determined, and this concentration was used for all subsequent tests.

3.2. Differentially expression of miRNAs and mRNAs

We identified 76 differentially expressed miRNAs following ACD treatment of Hep G2 cells, including 33 upregulated and 43 downregulated miRNAs ($|\log2FC| \geq 2$; q-value ≤ 0.05; Fig. 2a). The outcomes of the gene clustering analysis results are displayed in Fig. 2b. Similarly, a significant alteration in expression of 17 miRNAs occurred after ACD treatment. These include hsa-miR-4485-3p, hsa-miR-214-3p, hsa-miR-4732-3p, hsa-miR-12136, hsa-miR-1307-5p, hsa-miR-4484, has-miR-26a-1-3p, hsa-miR-191-3p, hsa-miR-486-5p, hsa-miR-92a-1-5p, hsa-miR-133a-3p, hsa-miR-4488, and hsa-miR-26a-2-3p (Table 1). Based on these results, it was clear

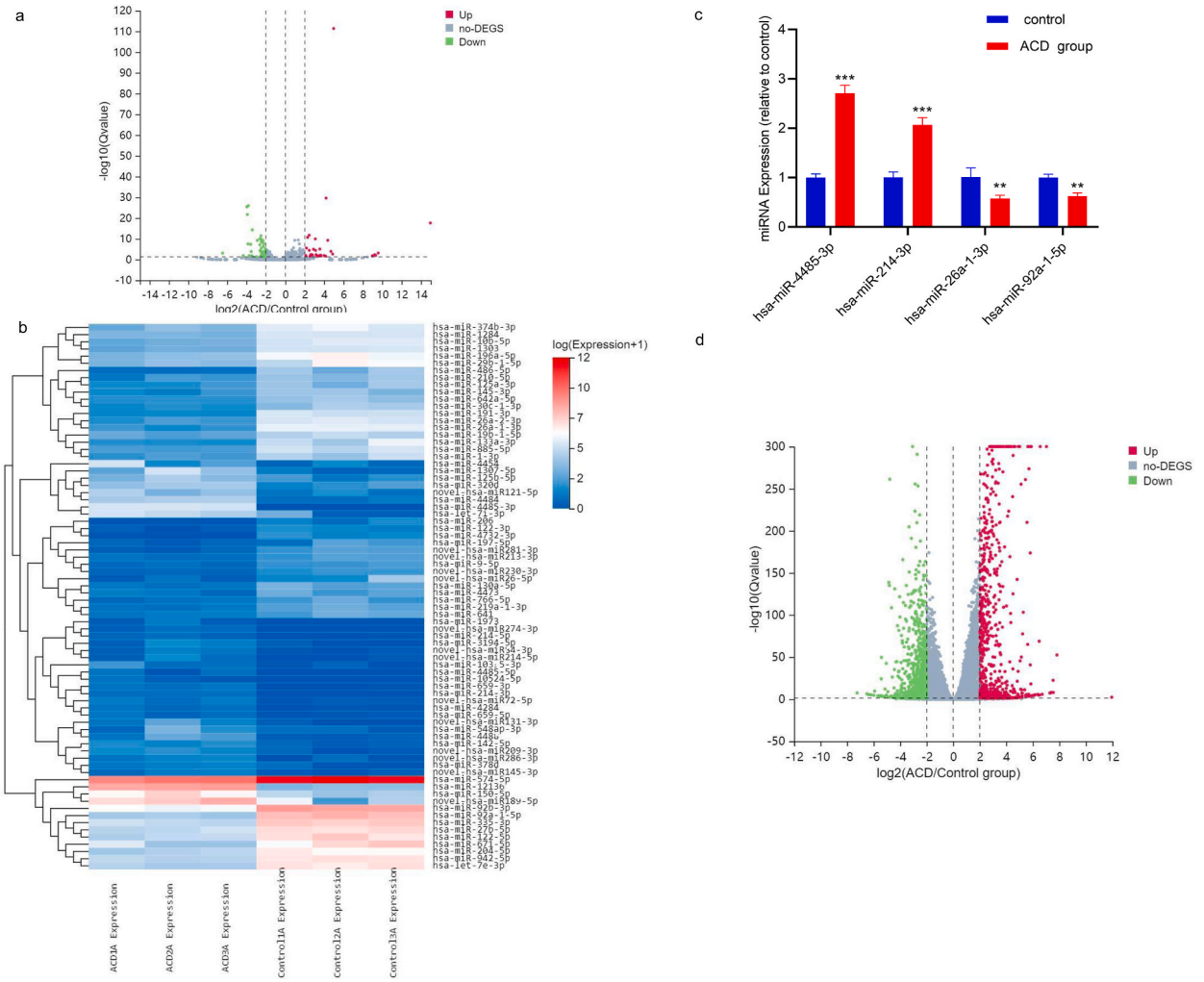

Fig. 2. Libraries analysed for the expression of miRNAs and mRNAs. (a) Volcano plot of differentially expressed mature miRNAs. The vertical lines represent the threshold for a relative expression fold-change of 2 or -2 relative to levels in the control group. The horizontal line represents the threshold q-value of 0.05. In HepG2 cells treated with ACD ($|\log_2FC| \geq 2$; q-value ≤ 0.05), the red spots in the top right sectors are considerably upregulated while the blue points in the top left sectors are significantly downregulated. (b) Heat map of differential expression of miRNAs in the experimental groups (c) Validation of a subset of miRNA sequencing results by qRT PCR. *U6* was used as a control for normalisation. Data represent the mean ± standard deviation (***P < 0.001, **P < 0.01). (d) Volcano plot of differentially expressed mRNAs. (For interpretation of the references to colour in this figure legend, the reader is referred to the Web version of this article.)

Table 1
Differentially expressed miRNAs between treated group cells and controls ($|\log_2 FC| \geq 3$; q-value ≤ 0.001).

miRNA	q-value	$\|\log_2 FC\|$	Type of regulation
hsa-miR-4485-3p	2.23E-18	14.96510786	Up
hsa-miR-214-3p	7.06E-04	9.579315938	Up
hsa-miR-4732-3p	7.96E-04	6.47438196	Down
hsa-miR-12136	4.26E-112	4.97724974	Up
novel-hsa-miR131-3p	1.12E-04	4.696588862	Up
hsa-miR-1307-5p	5.26E-10	4.372731829	Up
hsa-miR-4484	2.25E-30	4.199079984	Up
hsa-miR-26a-1-3p	3.86E-26	3.972967589	Down
hsa-miR-191-3p	1.94E-22	3.91230643	Down
hsa-miR-486-5p	2.74E-08	3.85395163	Down
hsa-miR-92a-1-5p	1.06E-26	3.808533639	Down
hsa-miR-133a-3p	4.60E-08	3.563718276	Down
hsa-miR-4488	8.53E-06	3.555879676	Up
novel-hsa-miR281-3p	1.44E-04	3.512731826	Down
hsa-miR-26a-2-3p	4.68E-15	3.404368422	Down
novel-hsa-miR209-3p	3.66E-05	3.110931991	Up
novel-hsa-miR121-5p	1.09E-10	3.087927141	Up

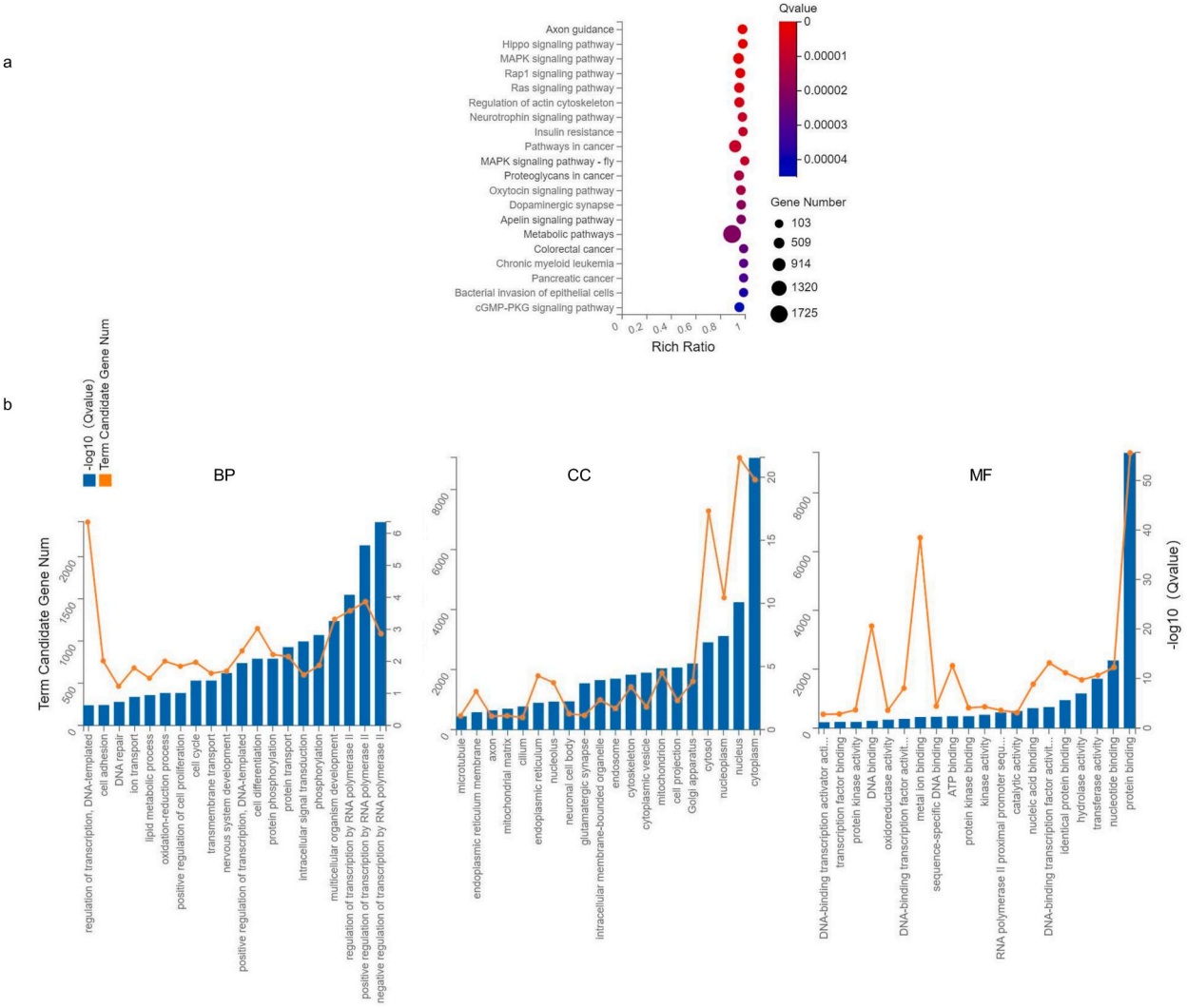

Fig. 3. Enrichment analysis of differentially expressed target genes. (a) Kyoto Encyclopaedia of Genes and Genomes pathway enrichment analysis of differentially expressed target genes. (b) Gene Ontology analysis based on the predicted targets of the differentially expressed miRNAs.

that the *A. chinensis* regulates miRNA expression in Hep G2 cells. However, further studies are needed to further confirm this. A total of 4 types of novel miRNAs with unknown function were also identified. To validate the outcomes of the sequencing data, qPCR was conducted to quantify the expression of miRNAs showing differential expression. For example, hsa-miR-4485-3p and hsa-miR-214-3p (Fig. 2c) were significantly upregulated in Hep G2 cells treated with ACD ($P < 0.001$), whereas hsa-miR-26a-1-3p and hsa-miR-92a-1-5p were downregulated. These outcomes confirmed the results of miRNA sequencing.

To assess the effects of miRNA changes on mRNA, variations in mRNA expression in the control and treatment groups were also analysed. A total of 1617 differentially expressed mRNAs were identified, which included 754 upregulated and 863 downregulated mRNAs ($|\log2FC| \geq 2$; q-value ≤ 0.05; Fig. 2d).

3.3. Target gene prediction and enrichment analysis

Among them, 17 miRNAs were found to have the most significant differential expression ($|\log2FC| \geq 3$, q-value ≤ 0.001). Therefore, we predicted the target genes of 17 significantly differentially expressed miRNAs, and 212 target genes were differentially expressed in the control and treatment groups ($|\log2FC| \geq 1$, q-value ≤ 0.05). Analysis of the KEGG pathways of the differentially target genes showed a close link with differentially enriched signalling pathways related to growth, cell cycle, and apoptosis of tumour cells. These include the axon guidance, Hippo, mitogen-activated protein kinase (MAPK), repressor/activator protein 1 (Rap1), and Ras signalling pathways (Fig. 3a). Apoptosis and cell cycle regulation are intimately associated with these signaling pathways.

The differentially expressed target genes underwent GO enrichment analysis (Fig. 3b). Diverse functional signalling pathways were enriched, such as those involved in protein binding, nucleotide binding, and transferase activity. Similarly, for biological processes and cellular components, transcription regulation by RNA polymerase II and cytoplasm were the most enriched GO terms, respectively.

3.4. Construction of a differentially expressed miRNA and target gene network

To clarify the targeting relationship between differentially expressed miRNAs and mRNA, a network map of 17 miRNAs and 212 mRNA was constructed to determine the targeted interactions. As shown in Fig. 4, among the miRNAs that target multiple genes, hsa-miR-4488 targeted the most significantly differentially expressed genes, including *ARC*, *HSPA6*, *C11orf86*, *PIP5KL1*, *GADD45B*,

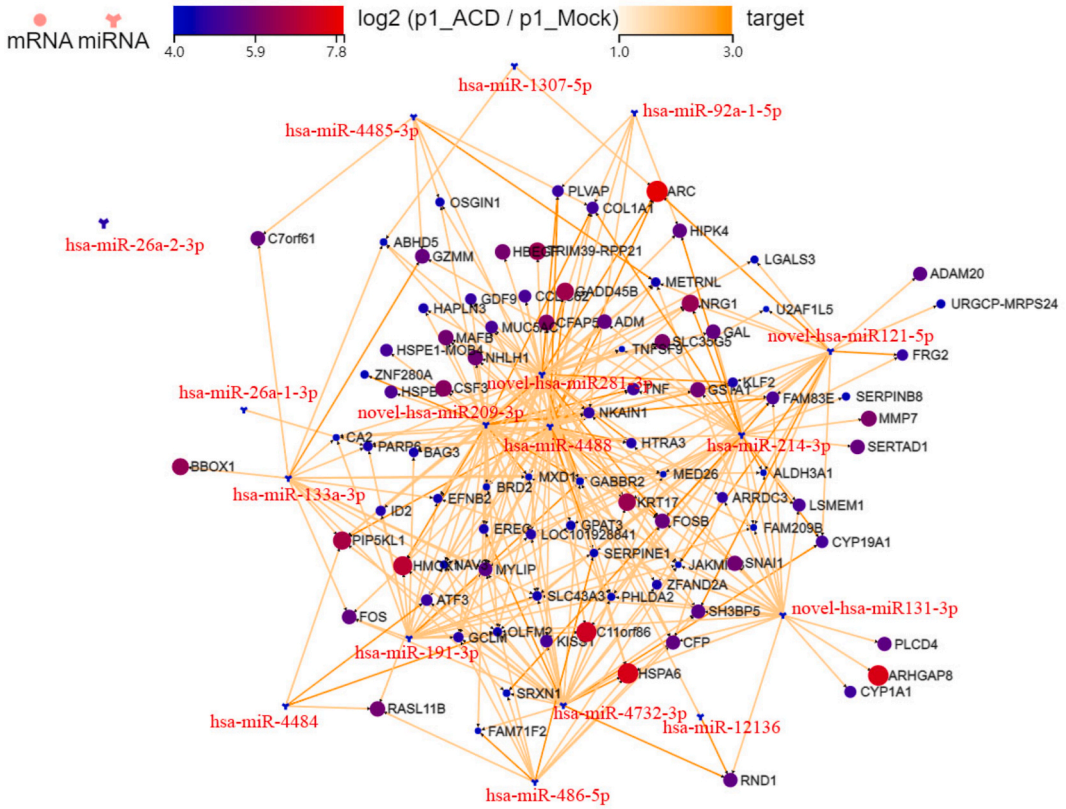

Fig. 4. Network representation of differentially expressed miRNAs and their target genes. Different shapes indicate different RNAs, and a deeper colour indicates a more significant difference in target gene expression. The yellow line indicates stronger targeting of miRNA. (For interpretation of the references to colour in this figure legend, the reader is referred to the Web version of this article.)

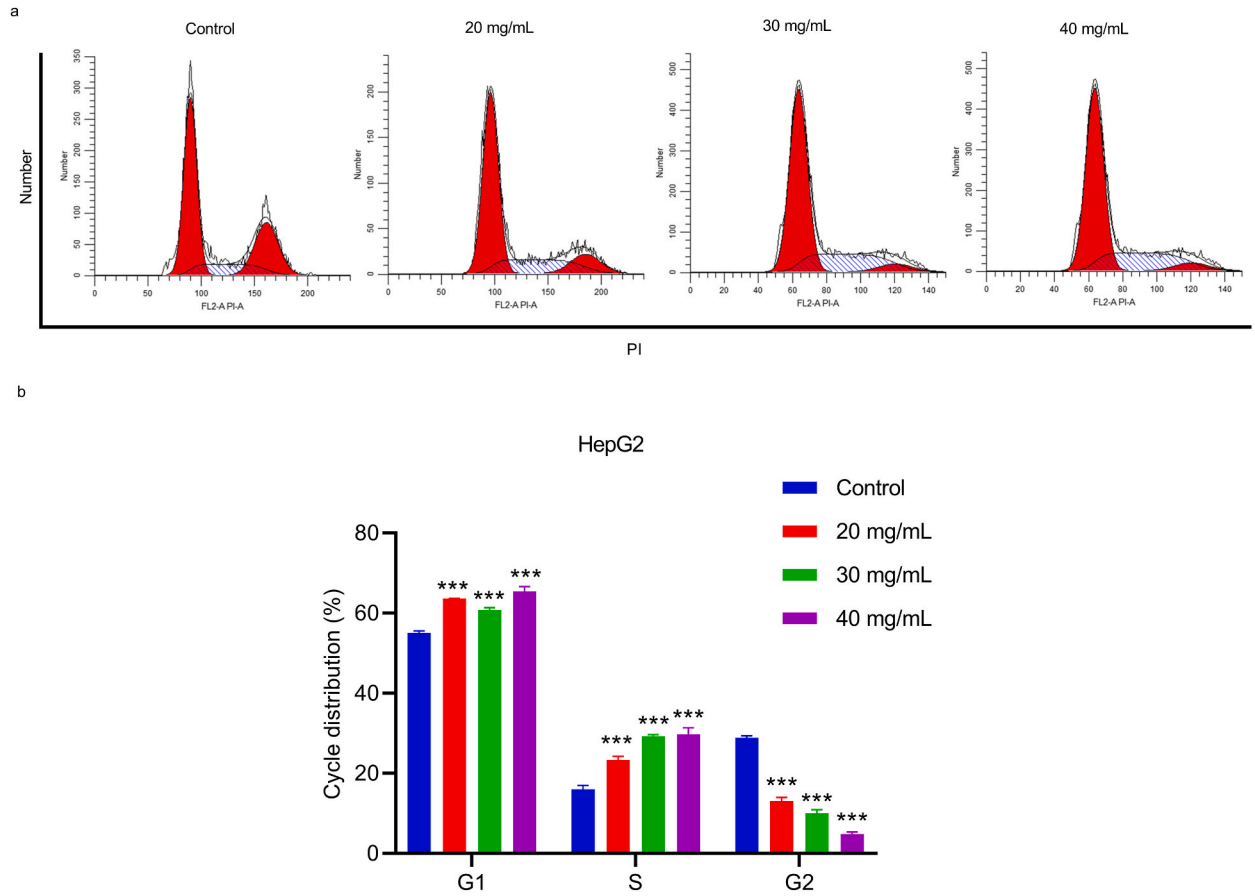

Fig. 5. In HepG2 cells, ACD influences the distribution of the cell cycle. (a) HepG2 cells were incubated with various concentrations of ACD (20–40 mg/mL) to analyze the cell cycle and (b) ACD-induced cell cycle arrest (***P 0.001).

KRT17, and *NRG1*; and hsa-miR-4732-3p targeted *HSPA6*, *HMOX1*, *PIP5KL1*, and *KRT17*. In turn, certain genes are targeted by multiple miRNAs. For example, the *ARC* gene is targeted by hsa-miR-1307-5p and hsa-miR-4488. Similarly, *HSPA6* is targeted by hsa-miR-4732-3p, hsa-miR-486-5p, and hsa-miR-4488, while *C11orf86* is targeted by hsa-miR-214-3p, hsa-miR-4732-3p, hsa-miR-191-3p, and hsa-miR-4488. Moreover, these target genes were significantly enriched in the axon guidance, Hippo, MAPK, Rap1, and Ras signalling pathways. Therefore, miRNAs possibly regulate target gene expression, thereby regulating the axon guidance, Hippo, MAPK, Rap1, and Ras signalling pathways to inhibit tumour cell growth.

3.5. Cell cycle phase effects of *A. chinensis*

The *A. chinensis* effect on the Hep G2 cell cycle revealed a substantially greater cell number in the G0/G1 phase of the ACD group than the control ($P < 0.001$). An increase in the cell number was also observed in the S phase ($P < 0.001$). In contrast, the quantity of cells in the G2/M phase was drastically reduced. These findings suggest that *A. chinensis* arrested the Hep G2 cell cycle at the G0/G1 and S phases (Fig. 5 a, b).

3.6. Effect of *A. chinensis* on the apoptosis rate

The apoptosis rate (including early and late apoptosis) of Hep G2 cells treated with different concentrations of ACD was significantly increased by flow cytometry analysis ($P < 0.001$) compared to control cells (Fig. 6 a, b). These results suggest that *A. chinensis* promotes apoptosis in Hep G2 cells.

3.7. Effect of *A. chinensis* on tumour growth in vivo

We further constructed a subcutaneously transplanted cancer model to examine the antitumor effects of *A. chinensis* (Fig. 7a and b). The ACD treatment significantly reduced the growth rate of tumour tissue compared to the control ($P < 0.001$). The growth rates of tumour tissue were lower in both the positive control and combination groups than the ACD group. These findings indicate that

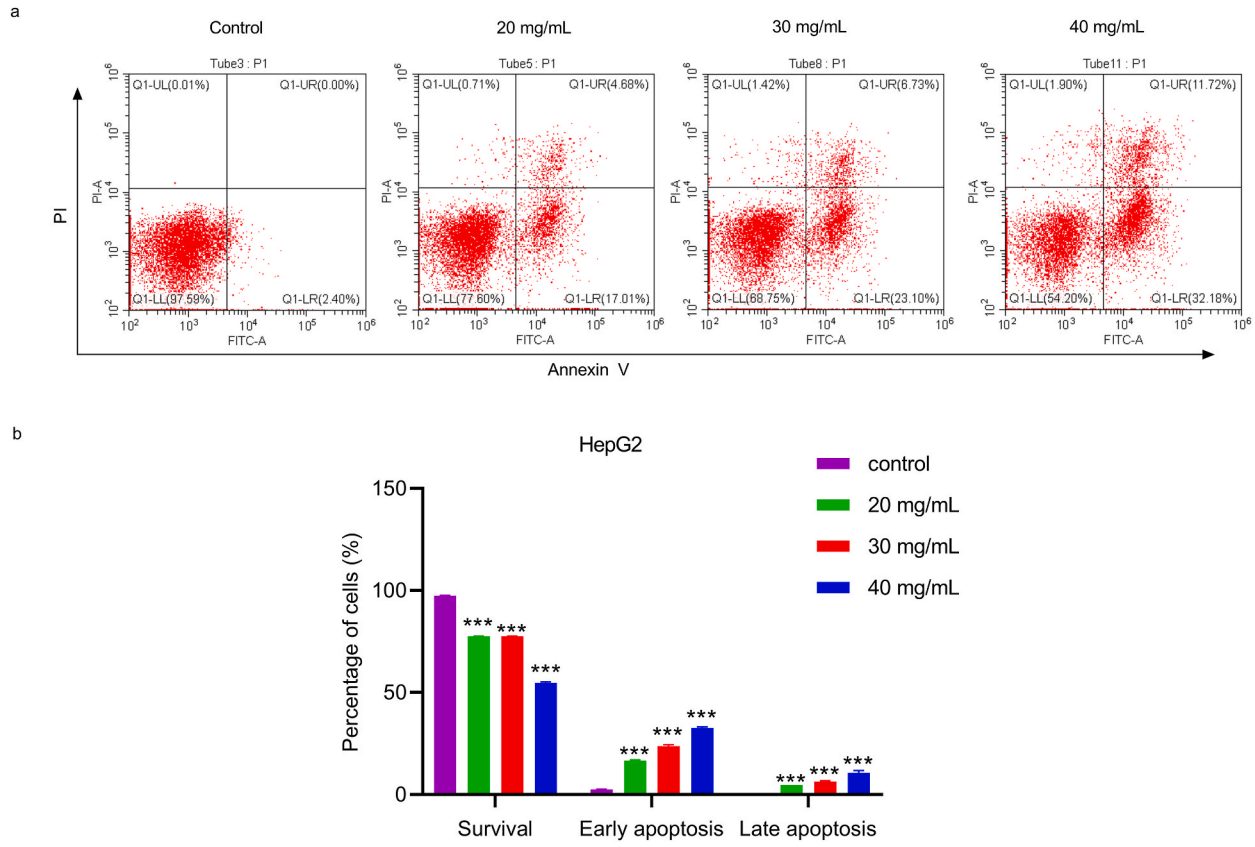

Fig. 6. ACD induces apoptosis in HepG2 cells. (a) HepG2 cells were treated for 24 h with the indicated concentrations (20–40 mg/mL) of ACD, and apoptosis was detected by Annexin V-FITC/propidium iodide double staining followed by flow cytometry. (b) Percentage of apoptotic cells (***$P < 0.001$).

A. chinensis has potent antitumor effects in *vivo.* Furthermore, no variation in BW was observed, indicating that *A. chinensis* had no effect on the mice BW (Fig. 7c).

4. Discussion

A. chinensis, a TCM-based insect with multiple medicinal properties, including anticancer activity, is of significant scientific and commercial interest. This insect has been applied to treat cancers due to its antibacterial, anticancer, and anticoagulant properties. However, the mechanisms underlying its inhibitory effects on HCC cells remain unknown. Our findings showed that *A. chinensis* profoundly inhibited of the proliferation of Hep G2 cells and ultimately promoted apoptosis through cell cycle arrest. In addition, we confirmed that *A. chinensis* inhibited the growth of mouse Hepa 1–6 cells *in vivo*. Further, changes in miRNA and mRNA expression profiles and their interactions in ACD-treated Hep G2 cells revealed the possible underlying molecular mechanisms of *A. chinensis* induced cell cycle arrest and apoptosis. Thus, the findings presented here establish a scientific foundation for the use and development of antitumor drugs including *A. chinensis.*

miRNAs regulate tumour growth by mediating the expression of target mRNAs and inhibiting protein translation [50]. The active ingredients used in TCM exert anticancer effects by regulating the expression of miRNA [51–53]. In Hep G2 cells treated with ACD, we identified 76 miRNAs with differentially expression, including 33 and 43 miRNAs with upregulated and downregulated expression, respectively. Among them, several miRNAs were found to be directly involved in the regulation of tumour growth. Similarly, breast cancer (MDA-MB-231) cells are inhibited by hsa-miR-4485-3p by inhibiting the expression of cell cycle factors cyclin B1 and D1 [54]. Also, hsa-miR-214-3p showed the same inhibitory effect on MDA-MB-231 cell growth, and its targets include *VDR*, *TSC22D1*, *ST6GAL1*, *CSF1*, *CDC73*, and *ARL2* [55]. miR-1307 binds to hsa_circ_0091570 and directly targets *ISM1* to promote HCC cell proliferation and migration while inhibiting HCC cell apoptosis [56]. hsa-miR-4488 targets genes closely associated to the cell cycle control, endoplasmic reticulum stress, and lipid signalling pathways [57]. Studies have found that the potential involvement of miR-4484 in the TGF signalling pathway increases the susceptibility of early cancer cells to apoptosis and cell cycle arrest [58,59]. However, some downregulated miRNAs also play regulatory roles in tumour growth. Among them, hsa-miR-4732-3p, which is the most downregulated miRNA, may synergistically regulate the cell cycle of oesophageal cancer [60]. Furthermore, hsa-miR-486-5p might regulate tumour progression through the epigenetic regulation of the MAPK signalling pathway [61]. These miRNAs inhibit tumour growth by

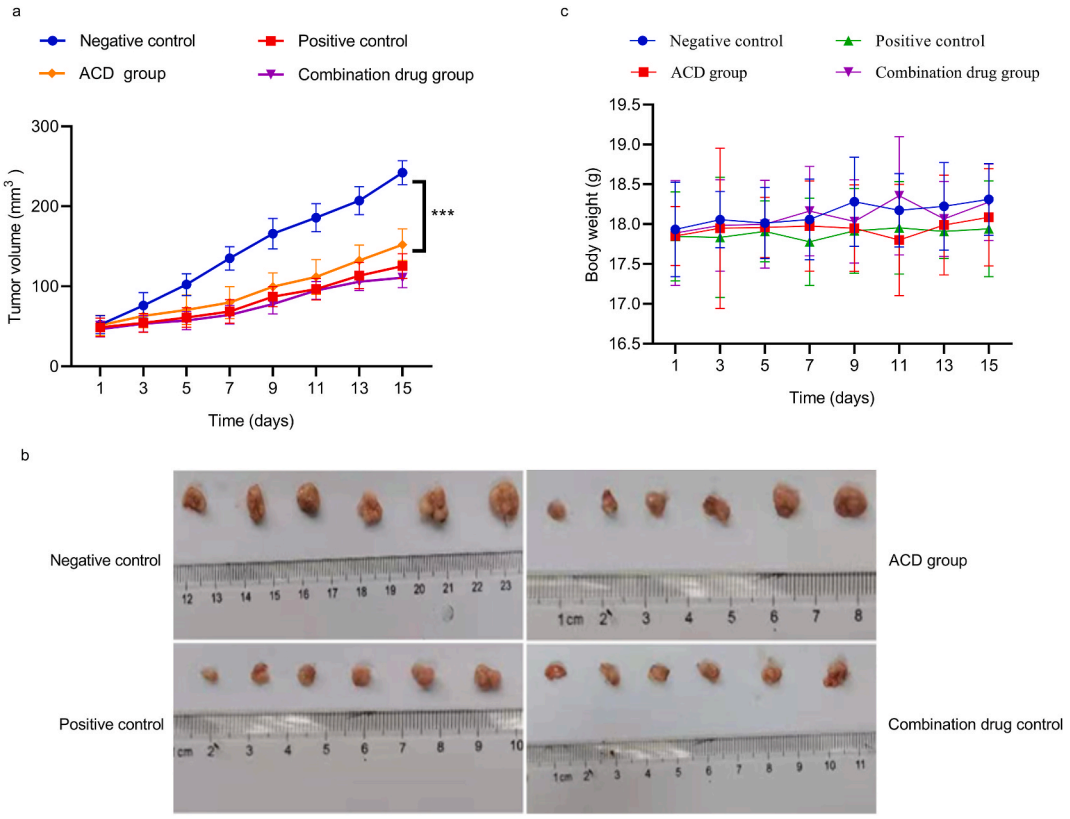

Fig. 7. Effects of ACD on Hepa1-6 tumour cell growth *in vivo*. (a) Growth curves of tumour tissues (***P < 0.001). (b) BW of Hepa1-6 cell-bearing mice were measured after treatment with ACD. (c) Images of tumour tissues.

targeting tumour cell proliferation and modulating the cell cycle, apoptosis, and target gene expression. Therefore, we hypothesised that *A. chinensis* might regulate the expression of target genes by acting on these differentially expressed miRNAs to regulate cell cycle- and apoptosis-related signalling pathways, thereby inhibiting the growth of Hep G2 cells.

The mRNA expression patterns of ACD-treated cells were compared with those of control cells to detect differential expressed genes. In total, 1617 genes were identified, comprising 754 upregulated and 863 downregulated mRNAs. The axon guidance, Hippo, MAPK, Rap1, and Ras signalling pathways showed a high enrichment of differentially expressed genes according to the KEGG pathway analysis. These pathways are closely related to the regulation of tumour cell proliferation, cell cycle, and apoptosis [62,63]. Furthermore, the local network diagram showed that multiple miRNAs regulated the expression of *ACR*, *HSPA6*, *HMOX1*, *C11orf86*, and *GADD45B*. There is evidence that these genes regulate tumour cell proliferation, cycle, and apoptosis-related signaling pathways [57,64,65]. Additionally, flow cytometry results confirmed that *A. chinensis* arrests the G0/G1 and S phases of Hep G2 cell cycle and induces apoptosis. Finally, we confirmed that ACD-treated HCC cells could not form robust tumours *in vivo*. In conclusion, *A. chinensis* might regulate the expression of *ACR*, *HSPA6*, *HMOX1*, *C11orf86*, *GADD45B*, and other target genes via hsa-miR-4485-3p, hsa--miR-214-3p, and hsa-miR-4732-3p, thereby inducing Hep G2 cell cycle arrest and activating apoptosis-related signalling pathways, resulting in HCC cell growth inhibition.

We demonstrated variations in miRNA and mRNA expression profiles and targeting between them in ACD-treated Hep G2 cells and further verified that *A. chinensis* has an inhibiting impact on the proliferation of Hep G2 cells. However, we have only predicted the possible molecular mechanisms involved. Future studies should verify the interactions among miRNA, mRNA, and related signalling pathways and clarify the molecular mechanisms by which *A. chinensis* inhibits tumour growth through miRNA-mediated regulation of mRNA.

Ethics declarations

This study was reviewed and approved by the Animal Care and Use Institutional Committee of Guizhou University, with the approval number: EAE-GZU-2022-E044.

Funding

This research was funded by National Natural Science Foundation of China, grant number NSFC 82160743; Guizhou Provincial

Science and Technology Projects, grant number Qiankehe Pingtai Rencai-GCC [2022]029-1;Guizhou Provincial Science and Technology Projects, grant number QKH-ZK [2023]504; Guizhou Provincial Science and Technology Projects, grant number QKH-ZK [2021]111; and Guizhou Province Graduate Research Fund, grant number YJSCXJH [2020]074.

Data availability statement

The datasets used and/or analysed during the current study are available from the corresponding author upon reasonable request. Raw sequencing data are available at the National Center for Biotechnology Information database under accession number PRJNA916295 (https://www.ncbi.nlm.nih.gov/sra/PRJNA989285).

CRediT authorship contribution statement

Renlian Cai: Writing – review & editing, Writing – original draft, Validation, Methodology, Funding acquisition, Formal analysis, Data curation. **Xumei Chen:** Writing – original draft, Validation, Formal analysis, Data curation. **Samiullah Khan:** Writing – review & editing, Writing – original draft, Methodology. **Haiyin Li:** Writing – review & editing, Validation. **Jun Tan:** Software, Methodology, Funding acquisition, Data curation. **Ying Tian:** Writing – original draft, Validation. **Shuai Zhao:** Writing – original draft, Investigation. **Zhiyong Yin:** Validation, Software. **Daochao Jin:** Writing – review & editing, Supervision, Project administration, Methodology, Investigation, Funding acquisition. **Jianjun Guo:** Writing – review & editing, Supervision, Project administration, Methodology, Investigation, Funding acquisition.

Declaration of competing interest

The authors declare that they have no known competing financial interests or personal relationships that could have appeared to influence the work reported in this paper.

References

[1] R. Cai, J. Tan, D. Fan, Research on medicinal and edible value of *Aspongopus chinensis* Dallas after being novelly processed, Journal of Zunyi Medical University 39 (2016) 345–349.
[2] J. Guo, J. Tan, C. Wei, Y. Feng, D. Jin, Overwintering conditions optimization of *Aspongopus chinensis*, J. Mountain Agric. Biol 38 (2019) 71–74.
[3] S. Zhao, J. Tan, H.M. Yu, Y. Tian, Y.F. Wu, R. Luo, J.J. Guo, In vivo and in vitro antiproliferative and antimetastatic effects of hemolymph of *Aspongopus chinensis* Dallas on breast cancer cell, J. Tradit. Chin. Med. 41 (2021) 523–529, https://doi.org/10.19852/j.cnki.jtcm.2021.03.004.
[4] T. Gong, J. Du, S.W. Li, H. Huang, X.L. Qi, Identification and functional analysis of a defensin CcDef2 from *Coridius chinensis*, Int. J. Mol. Sci. 23 (2022), https://doi.org/10.3390/ijms23052789.
[5] K. Xiong, F. Zeng, X. Lei, Y. Wei, X. Zhou, X. Hou, Modern pharmacological research and application of medicinal insect *Coridius chinensis*, Heliyon 10 (2024) e24613, https://doi.org/10.1016/j.heliyon.2024.e24613.
[6] X.M. Chen, S.Q. Zhang, M.L. Cao, J.J. Guo, R. Luo, Isolation of peptide inhibiting SGC-7901 cell proliferation from *Aspongopus chinensis* Dallas, Int. J. Mol. Sci. 23 (2022), https://doi.org/10.3390/ijms232012535.
[7] E. Zhang, X. Ji, F. Ouyang, Y. Lei, S. Deng, H. Rong, X. Deng, H. Shen, A minireview of the medicinal and edible insects from the traditional Chinese medicine (TCM), Front. Pharmacol. 14 (2023) 1125600.
[8] S. Li, L. Li, H.B. Peng, X.J. Ma, L.Q. Huang, J. Li, Advances in studies on chemical constituents, pharmacological effects and clinical application of *Aspongopus chinensis*, Zhongguo Zhongyao Zazhi 45 (2020) 303–311, https://doi.org/10.19540/j.cnki.cjcmm.20190829.202.
[9] H. Sheridan, B. Kopp, L. Krenn, D. Guo, J. Sendker, Traditional Chinese herbal medicine preparation: invoking the butterfly effect, Science 350 (2015) S64–S66.
[10] Y. Tian, J. Tan, S. Zhao, J.J. Guo, Main components and anti-proliferative activities of *Aspongopus Chinensis* decoction on breast cancer cells, J Environ EntomolJ Environ Entomol 42 (2020) 299–305 (in Chinese).
[11] S. Yang, R.L. Cai, X.M. Chen, Z. S, Y. Tian, J.J. Guo, Effect of *Aspongopus Chinensis* decoction on the growth of hepatoma cells Hepg2 in vitro, J Mt Agric Biol 41 (2022) 74–79 (in Chinese).
[12] Z. He, L. Zhang, L. Lin, Z. Sun, X. Hou, Protection of stink-bug on manganese-induced reproductive damage to male rats, Chin. Tradit. Pat. Med. 38 (2016) 258–261.
[13] Q. Liu, C. Cen, H. Fu, F. Wang, Y. Wang, T. Xu, X. Hou, Antioxidant activity of *Coridius chinensis* extracts on manganese-induced testicular damage in rats, Environ. Toxicol. 34 (2019) 1067–1073.
[14] J. Tan, Y. Tian, R. Cai, R. Luo, J. Guo, Chemical composition and antiproliferative effects of a methanol extract of *Aspongopus chinensis* Dallas, Evidence-based complementary and alternative medicine, eCAM 2019 (2019) 2607086, https://doi.org/10.1155/2019/2607086.
[15] J. Tan, Y. Tian, R. Cai, T. Yi, D. Jin, J. Guo, Antiproliferative and proapoptotic effects of a protein component purified from *Aspongopus chinensis* Dallas on cancer cells in vitro and in vivo, Evidence-based complementary and alternative medicine, eCAM 2019 (2019) 8934794, https://doi.org/10.1155/2019/8934794.
[16] Y.-N. Shi, Z.-C. Tu, X.-L. Wang, Y.-M. Yan, P. Fang, Z.-L. Zuo, B. Hou, T.-H. Yang, Y.-X. Cheng, Bioactive compounds from the insect *Aspongopus chinensis*, Bioorg. Med. Chem. Lett 24 (2014) 5164–5169.
[17] L. Liao, Y.-M. Yan, T. Xu, H.-L. Xia, Y.-X. Cheng, A pair of novel sulfonyl-containing N-acetyldopamine dimeric enantiomers from *Aspongopus chinensis*, Nat. Prod. Commun. 15 (2020) 1934578X20911270.
[18] H. Rumgay, M. Arnold, J. Ferlay, O. Lesi, C.J. Cabasag, J. Vignat, M. Laversanne, K.A. McGlynn, I. Soerjomataram, Global burden of primary liver cancer in 2020 and predictions to 2040, J. Hepatol. 77 (2022) 1598–1606, https://doi.org/10.1016/j.jhep.2022.08.021.
[19] A. Forner, M. Reig, J. Bruix, Hepatocellular carcinoma, Lancet 391 (2018) 1301–1314, https://doi.org/10.1016/s0140-6736(18)30010-2.
[20] M. Reig, A. Forner, J. Rimola, J. Ferrer-Fàbrega, M. Burrel, Á. Garcia-Criado, R.K. Kelley, P.R. Galle, V. Mazzaferro, R. Salem, B. Sangro, A.G. Singal, A. Vogel, J. Fuster, C. Ayuso, J. Bruix, BCLC strategy for prognosis prediction and treatment recommendation: the 2022 update, J. Hepatol. 76 (2022) 681–693.
[21] Z. Ren, J. Xu, Y. Bai, A. Xu, S. Cang, C. Du, Q. Li, Y. Lu, Y. Chen, Y. Guo, Z. Chen, B. Liu, W. Jia, J. Wu, J. Wang, G. Shao, B. Zhang, Y. Shan, Z. Meng, J. Wu, S. Gu, W. Yang, C. Liu, X. Shi, Z. Gao, T. Yin, J. Cui, M. Huang, B. Xing, Y. Mao, G. Teng, Y. Qin, J. Wang, F. Xia, G. Yin, Y. Yang, M. Chen, Y. Wang, H. Zhou, J. Fan, Sintilimab plus a bevacizumab biosimilar (IBI305) versus sorafenib in unresectable hepatocellular carcinoma (ORIENT-32): a randomised, open-label, phase 2-3 study, the Lancet, Oncology 22 (2021) 977–990, https://doi.org/10.1016/s1470-2045(21)00252-7.
[22] Y. Zhang, Z. Wu, H. Yu, H. Wang, G. Liu, S. Wang, X. Ji, Chinese herbal medicine wenxia changfu formula reverses cell adhesion-mediated drug resistance via the integrin β1-PI3K-AKT pathway in lung cancer, J. Cancer 10 (2019) 293–304, https://doi.org/10.7150/jca.25163.

[23] H. Sung, J. Ferlay, R.L. Siegel, M. Laversanne, I. Soerjomataram, A. Jemal, F. Bray, Global cancer statistics 2020: GLOBOCAN estimates of incidence and mortality worldwide for 36 cancers in 185 countries, CA A Cancer J. Clin. 71 (2021) 209–249.
[24] Z. Yan, Z. Lai, J. Lin, Anticancer properties of traditional Chinese medicine, Comb. Chem. High Throughput Screen. 20 (2017) 423–429.
[25] Z. Ma, Y. Fan, Y. Wu, D. Kebebe, B. Zhang, P. Lu, J. Pi, Z. Liu, Traditional Chinese medicine-combination therapies utilizing nanotechnology-based targeted delivery systems: a new strategy for antitumor treatment, Int. J. Nanomed. (2019) 2029–2053.
[26] D.P. Bartel, MicroRNAs: genomics, biogenesis, mechanism, and function, Cell 116 (2004) 281–297, https://doi.org/10.1016/s0092-8674(04)00045-5.
[27] H. Dong, J. Lei, L. Ding, Y. Wen, H. Ju, X. Zhang, MicroRNA: function, detection, and bioanalysis, Chem. Rev. 113 (2013) 6207–6233, https://doi.org/10.1021/cr300362f.
[28] J.-Y. Roignant, M. Soller, m6A in mRNA: an ancient mechanism for fine-tuning gene expression, Trends Genet. 33 (2017) 380–390.
[29] E. O'Day, A. Lal, MicroRNAs and their target gene networks in breast cancer, Breast Cancer Res. 12 (2010) 1–10.
[30] X. Wang, P. Yan, L. Liu, Y. Luo, L. Zhao, H. Liu, Q. Tang, K. Long, L. Jin, J. Ma, MicroRNA expression profiling reveals potential roles for microRNA in the liver during pigeon (Columba livia) development, Poultry Sci. 99 (2020) 6378–6389.
[31] R. Sunkar, V. Chinnusamy, J. Zhu, J.-K. Zhu, Small RNAs as big players in plant abiotic stress responses and nutrient deprivation, Trends Plant Sci. 12 (2007) 301–309.
[32] P. Brodersen, O. Voinnet, The diversity of RNA silencing pathways in plants, Trends Genet. 22 (2006) 268–280.
[33] H. Hwang, J. Mendell, MicroRNAs in cell proliferation, cell death, and tumorigenesis, Br. J. Cancer 94 (2006) 776–780.
[34] X. Xue, X. Fei, W. Hou, Y. Zhang, L. Liu, R. Hu, miR-342-3p suppresses cell proliferation and migration by targeting AGR2 in non-small cell lung cancer, Cancer Lett. 412 (2018) 170–178, https://doi.org/10.1016/j.canlet.2017.10.024.
[35] Y. Zhu, J. Gu, Y. Li, C. Peng, M. Shi, X. Wang, G. Wei, O. Ge, D. Wang, B. Zhang, J. Wu, Y. Zhong, B. Shen, H. Chen, MiR-17-5p enhances pancreatic cancer proliferation by altering cell cycle profiles via disruption of RBL2/E2F4-repressing complexes, Cancer Lett. 412 (2018) 59–68, https://doi.org/10.1016/j.canlet.2017.09.044.
[36] I. Grammatikakis, M. Gorospe, K. Abdelmohsen, Modulation of cancer traits by tumor suppressor microRNAs, Int. J. Mol. Sci. 14 (2013) 1822–1842, https://doi.org/10.3390/ijms14011822.
[37] T. Jiang, Z. Yin, R. Cai, H. Yu, Q. Lu, S. Zhao, Y. Tian, Y. Yan, J. Guo, X. Chen, Chromosomal-level genome assembly of a true bug, *Aspongopus chinensis* Dallas, 1851 (Hemiptera: Dinidoridae), Genome Biol Evol 13 (2021), https://doi.org/10.1093/gbe/evab232.
[38] T.J. Tian Y, S. Zhao, et al., Main components and anti-proliferative activities of *Aspongopus chinensis* decoction on breast cancer cells, J. Environ. Entomol 42 (2020) 299–305.
[39] M. Roy, G. Jin, J.H. Pan, D. Seoa, Y. Hwang, S. Oh, M. Lee, Y.J. Kim, S. Seo, Staining-free cell viability measurement technique using lens-free shadow imaging platform, Sens. Actuator B-Chem. 224 (2016) 577–583, https://doi.org/10.1016/j.snb.2015.10.097.
[40] B. Langmead, S.L. Salzberg, Fast gapped-read alignment with Bowtie 2, Nat. Methods 9 (2012) 357–359, https://doi.org/10.1038/nmeth.1923.
[41] M.I. Love, W. Huber, S. Anders, Moderated estimation of fold change and dispersion for RNA-seq data with DESeq2, Genome Biol. 15 (2014) 550, https://doi.org/10.1186/s13059-014-0550-8.
[42] M. Rehmsmeier, P. Steffen, M. Hochsmann, R. Giegerich, Fast and effective prediction of microRNA/target duplexes, RNA (New York, N.Y.) 10 (2004) 1507–1517, https://doi.org/10.1261/rna.5248604.
[43] V. Agarwal, G.W. Bell, J.W. Nam, D.P. Bartel, Predicting effective microRNA target sites in mammalian mRNAs, Elife 4 (2015), https://doi.org/10.7554/eLife.05005.
[44] A.J. Enright, B. John, U. Gaul, T. Tuschl, C. Sander, D.S. Marks, MicroRNA targets in Drosophila, Genome Biol. 5 (2003) R1, https://doi.org/10.1186/gb-2003-5-1-r1.
[45] H.J. Fu, J. Zhu, M. Yang, Z.Y. Zhang, Y. Tie, H. Jiang, Z.X. Sun, X.F. Zheng, A novel method to monitor the expression of microRNAs, Mol. Biotechnol. 32 (2006) 197–204, https://doi.org/10.1385/mb:32:3:197.
[46] Z. Chen, S. Shen, B. Peng, J. Tao, Intratumoural GM-CSF microspheres and CTLA-4 blockade enhance the antitumour immunity induced by thermal ablation in a subcutaneous murine hepatoma model, Int. J. Hyperther. 25 (2009) 374–382, https://doi.org/10.1080/02656730902976807.
[47] F.M. Gu, Q.L. Li, Q. Gao, J.H. Jiang, X.Y. Huang, J.F. Pan, J. Fan, J. Zhou, Sorafenib inhibits growth and metastasis of hepatocellular carcinoma by blocking STAT3, World J. Gastroenterol. 17 (2011) 3922–3932, https://doi.org/10.3748/wjg.v17.i34.3922.
[48] A. Baschnagel, A. Russo, W.E. Burgan, D. Carter, K. Beam, D. Palmieri, P.S. Steeg, P. Tofilon, K. Camphausen, Vorinostat enhances the radiosensitivity of a breast cancer brain metastatic cell line grown in vitro and as intracranial xenografts, Mol. Cancer Therapeut. 8 (2009) 1589–1595, https://doi.org/10.1158/1535-7163.Mct-09-0038.
[49] C. Jiang, R. Xu, X.X. Li, Y.F. Zhou, X.Y. Xu, Y. Yang, H.Y. Wang, X.F.S. Zheng, Sorafenib and carfilzomib synergistically inhibit the proliferation, survival, and metastasis of hepatocellular carcinoma, Mol. Cancer Therapeut. 17 (2018) 2610–2621, https://doi.org/10.1158/1535-7163.Mct-17-0541.
[50] I. Berindan-Neagoe, G.A. Calin, Molecular pathways: microRNAs, cancer cells, and microenvironment, Clin. Cancer Res. 20 (2014) 6247–6253, https://doi.org/10.1158/1078-0432.Ccr-13-2500.
[51] H.X. Deng, Y.Y. Yu, A.Q. Zhou, J.L. Zhu, L.N. Luo, W.Q. Chen, L. Hu, G.X. Chen, Yangzheng Sanjie decoction regulates proliferation and apoptosis of gastric cancer cells by enhancing let-7a expression, World J. Gastroenterol. 23 (2017) 5538–5548, https://doi.org/10.3748/wjg.v23.i30.5538.
[52] J. Guo, X. Li, L. Miao, H. Sun, X. Gao, S. Guo, Y. Zhang, P. Cong, W. Chen, High-throughput sequencing reveals the differential microRNA expression profiles of human gastric cancer SGC7901 cell xenograft nude mouse models treated with traditional Chinese medicine Si Jun Zi Tang decoction, Evidence-based complementary and alternative medicine, eCAM 2021 (2021) 6119212, https://doi.org/10.1155/2021/6119212.
[53] P. Liu, X. Yang, H. Zhang, J. Pu, K. Wei, Analysis of change in microRNA expression profiles of lung cancer A549 cells treated with Radix tetrastigma hemsleyani flavonoids, OncoTargets Ther. 11 (2018) 4283–4300, https://doi.org/10.2147/ott.S164276.
[54] C. Fitzpatrick, M.F. Bendek, M. Briones, N. Farfán, V.A. Silva, G. Nardocci, M. Montecino, A. Boland, J.F. Deleuze, J. Villegas, C. Villota, V. Silva, L. Lobos-Gonzalez, V. Borgna, E. Barrey, L.O. Burzio, V.A. Burzio, Mitochondrial ncRNA targeting induces cell cycle arrest and tumor growth inhibition of MDA-MB-231 breast cancer cells through reduction of key cell cycle progression factors, Cell Death Dis. 10 (2019) 423, https://doi.org/10.1038/s41419-019-1649-3.
[55] R. Elango, K.A. Alsaleh, R. Vishnubalaji, M. Manikandan, A.M. Ali, N. Abd El-Aziz, A. Altheyab, A. Al-Rikabi, M. Alfayez, A. Aldahmash, N.M. Alajez, MicroRNA expression profiling on paired primary and lymph node metastatic breast cancer revealed distinct microRNA profile associated with LNM, Front. Oncol. 10 (2020) 756, https://doi.org/10.3389/fonc.2020.00756.
[56] Y.G. Wang, T. Wang, M. Ding, S.H. Xiang, M. Shi, B. Zhai, hsa_circ_0091570 acts as a ceRNA to suppress hepatocellular cancer progression by sponging hsa-miR-1307, Cancer Lett. 460 (2019) 128–138, https://doi.org/10.1016/j.canlet.2019.06.007.
[57] S. Arumugam, B. Mary, M. Kumar, G.R. Jayandharan, Analysis of hepatic and retinal cell microRNAome during AAV infection reveals their diverse impact on viral transduction and cellular physiology, Gene 724 (2020) 144157, https://doi.org/10.1016/j.gene.2019.144157.
[58] S. Colak, P. Ten Dijke, Targeting TGF-β signaling in cancer, Trends in cancer 3 (2017) 56–71, https://doi.org/10.1016/j.trecan.2016.11.008.
[59] M. Rusek, M. Michalska-Jakubus, M. Kowal, J. Bełtowski, D. Krasowska, A novel miRNA-4484 is up-regulated on microarray and associated with increased MMP-21 expression in serum of systemic sclerosis patients, Sci. Rep. 9 (2019) 14264, https://doi.org/10.1038/s41598-019-50695-y.
[60] Z. Gao, R. Liu, J. Liao, M. Yang, E. Pan, L. Yin, Y. Pu, Possible tumor suppressive role of the miR-144/451 cluster in esophageal carcinoma as determined by principal component regression analysis, Mol. Med. Rep. 14 (2016) 3805–3813, https://doi.org/10.3892/mmr.2016.5691.
[61] L. Lyu, H. Li, C. Chen, Y. Yu, L. Wang, S. Yin, Y. Hu, S. Jiang, F. Ye, P. Zhou, Exosomal miRNA profiling is a potential screening route for non-functional pituitary adenoma, Front. Cell Dev. Biol. 9 (2021) 771354, https://doi.org/10.3389/fcell.2021.771354.
[62] D. Reddy, R. Kumavath, P. Ghosh, D. Barh, Lanatoside C induces G2/M cell cycle arrest and suppresses cancer cell growth by attenuating MAPK, Wnt, JAK-STAT, and PI3K/AKT/mTOR signaling pathways, Biomolecules 9 (2019), https://doi.org/10.3390/biom9120792.
[63] F. Sanchez-Vega, M. Mina, J. Armenia, W.K. Chatila, A. Luna, K.C. La, S. Dimitriadoy, D.L. Liu, H.S. Kantheti, S. Saghafinia, D. Chakravarty, F. Daian, Q. Gao, M. H. Bailey, W.W. Liang, S.M. Foltz, I. Shmulevich, L. Ding, Z. Heins, A. Ochoa, B. Gross, J. Gao, H. Zhang, R. Kundra, C. Kandoth, I. Bahceci, L. Dervishi,

U. Dogrusoz, W. Zhou, H. Shen, P.W. Laird, G.P. Way, C.S. Greene, H. Liang, Y. Xiao, C. Wang, A. Iavarone, A.H. Berger, T.G. Bivona, A.J. Lazar, G.D. Hammer, T. Giordano, L.N. Kwong, G. McArthur, C. Huang, A.D. Tward, M.J. Frederick, F. McCormick, M. Meyerson, E.M. Van Allen, A.D. Cherniack, G. Ciriello, C. Sander, N. Schultz, Oncogenic signaling pathways in the cancer genome atlas, Cell 173 (2018) e310, https://doi.org/10.1016/j.cell.2018.03.035, 321-337.

[64] S. Crimi, L. Falzone, G. Gattuso, C.M. Grillo, S. Candido, A. Bianchi, M. Libra, Droplet digital PCR analysis of liquid biopsy samples unveils the diagnostic role of hsa-miR-133a-3p and hsa-miR-375-3p in oral cancer, Biology 9 (2020), https://doi.org/10.3390/biology9110379.

[65] C.T. Xiao, W.J. Lai, W.A. Zhu, H. Wang, MicroRNA derived from circulating exosomes as noninvasive biomarkers for diagnosing renal cell carcinoma, OncoTargets Ther. 13 (2020) 10765–10774, https://doi.org/10.2147/ott.S271606.